Detecting weak magnetic fields in the central stars of planetary nebulae

Steffen M.[1], Hubrig S.[1], Todt H.[2], Schöller M.[3], Sandin C.[1], Hamann W.-R.[2], Schönberner D.[1]

[1]*Leibniz-Institut für Astrophysik Potsdam, Potsdam, Germany, email:* `msteffen@aip.de`
[2]*Institut für Physik und Astronomie, Universität Potsdam, Germany*
[3]*European Southern Observatory, Garching, Germany*

Abstract We have carried out low-resolution spectropolarimetric observations with FORS 2, installed on the VLT, ESO, of a representative sample of 12 bright central stars of Planetary Nebulae (PNe) with different morphology. Two of the sample are hydrogen-deficient (Wolf-Rayet type) stars. Our measurements rule out the existence of strong global magnetic fields of the order of kG in any of the PN central stars of our sample. Even so, our data may indicate the presence of weak mean longitudinal magnetic fields of a few hundred Gauss in the central stars of two elliptical nebulae, IC 418 and NGC 2392, and a very weak magnetic field of about 100 G in the Wolf-Rayet type central star Hen 2-113. However, the significance of these marginal detections depends on the method adopted for estimating the uncertainties in the magnetic-field measurements.

1. Introduction

One of the major open questions regarding the formation of Planetary Nebulae (PNe) concerns the origin of their non-spherical, often axisymmetric, shapes (e.g. [1]). A combination of stellar rotation and magnetic fields [4] is an attractive alternative to the more popular binary hypothesis (e.g. [3]), but very little is known so far about the rotation rates and surface magnetic fields of the central stars of PNe. In principle, the role of magnetic fields in shaping PNe may be verified – or disproved – by empirical evidence, by measuring the magnetic field in a representative sample of central stars. The first claims of detections of kG magnetic fields in two central stars of PNe, observed with FORS 1 in spectropolarimetric mode [8], could not be confirmed by improved analysis methods [9] and new measurements [10]. This paper presents our own analysis, which is based on a larger sample of stars and observed with the superior sensitivity of FORS 2.

2. FORS 2 spectropolarimetric observations

Spectropolarimetric observations of the twelve central stars were carried out between 2011 October 5 and 2012 March 28 in service mode at ESO, using FORS 2 on the 8-m Antu telescope of the VLT. This multi-mode instrument is

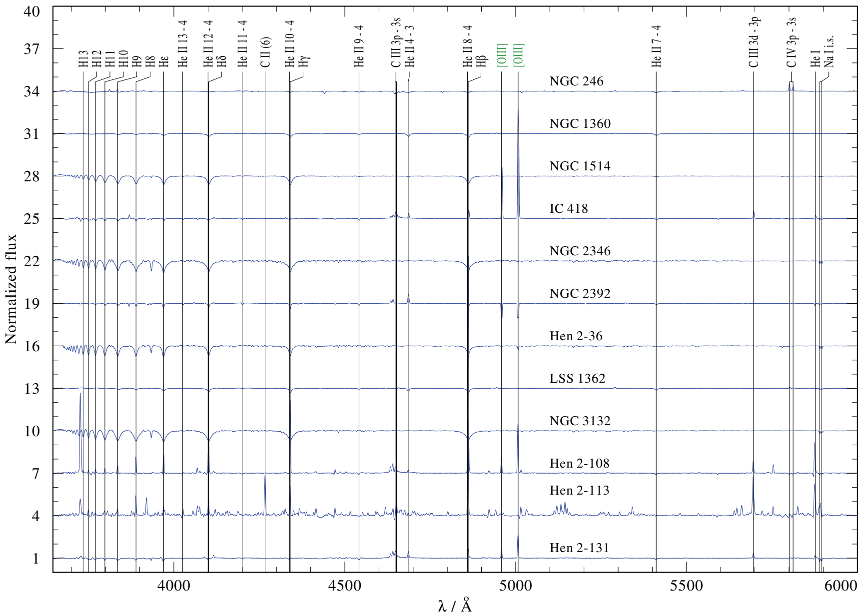

Figure 1. Normalized FORS 2 Stokes I spectra of the 12 central stars in our sample, displayed with vertical offsets of 3 units between adjacent spectra. The strongest spectral lines are identified. The spectra of NGC 1514, NGC 2346, Hen 2-26, and NGC 3132 are dominated by an A-type companion.

equipped with polarization analyzing optics, comprised of super-achromatic half-wave and quarter-wave phase retarder plates, and a Wollaston prism with a beam divergence of $22''$ in standard resolution mode. For the observations we used a slit-width of $0.5''$ and the GRISM 600B in order to achieve a spectral resolving power of about 1650.

Normalized FORS 2 Stokes I spectra of all the sample stars are displayed in Fig. 1, and include identifications of certain spectral lines. The signal-to-noise ratio of the Stokes I spectra ranged from $S/N \approx 800$ for the faintest central star (Hen 2-108, $m_{\rm V} = 12.72$) to $S/N \approx 2000$ for the brightest target (NGC 1514, $m_{\rm V} = 9.42$). For the analysis described below, we used the original wavelength scale provided by the ESO pipeline ($\Delta\lambda = 0.75$ Å) and avoided interpolation to finer wavelength steps.

3. Magnetic field measurements

A detailed description of the procedure of determining a mean longitudinal magnetic field, $\langle B_\mathrm{z} \rangle$, from FORS 2 spectropolarimetric observations has been presented elsewhere (e.g. [6, 7], and references therein). In brief, $\langle B_\mathrm{z} \rangle$ is derived from the relation

$$y(\lambda) \equiv \frac{V}{I} = -\frac{g_\mathrm{eff}\, e \lambda^2}{4\pi m_\mathrm{e} c^2} \frac{1}{I} \frac{\mathrm{d}I}{\mathrm{d}\lambda} \langle B_\mathrm{z} \rangle \equiv x(\lambda)\, \langle B_\mathrm{z} \rangle \,, \tag{1}$$

where V is the Stokes parameter that measures the circular polarization, I the intensity of the unpolarized spectrum, g_eff the effective Landé factor, e the electron charge, m_e the electron mass, c the speed of light, λ the wavelength, $\mathrm{d}I/\mathrm{d}\lambda$ the wavelength derivative of Stokes I, and $\langle B_\mathrm{z} \rangle$ the mean longitudinal (line-of-sight) magnetic field. From the dataset $\{x_i(\lambda), y_i(\lambda)\}_{i=1,N}$, where N is the total number of considered spectral bins, assuming that the relation (1) is valid both for absorption and emission lines, and adopting $g_\mathrm{eff} = 1$, one computes $\langle B_\mathrm{z} \rangle$ from linear regression (e.g. [11]):

$$\langle B_\mathrm{z} \rangle = \frac{\overline{xy} - \overline{x}\,\overline{y}}{\overline{x^2} - \overline{x}^2}, \tag{2}$$

where we have defined

$$\overline{x} = \frac{\sum_N w_i x_i}{\sum_N w_i},\ \ \overline{x^2} = \frac{\sum_N w_i x_i^2}{\sum_N w_i},\ \ \overline{y} = \frac{\sum_N w_i y_i}{\sum_N w_i},\ \ \overline{xy} = \frac{\sum_N w_i x_i y_i}{\sum_N w_i}\,. \tag{3}$$

The weight for each pixel is given by its signal-to-noise ratio as $w_i = (S/N)_i^2$. By considering the propagation of errors, we calculated the $1\,\sigma$ uncertainty of $\langle B_\mathrm{z} \rangle$ from

$$\sigma_B = \sqrt{\frac{1}{\sum_N w_i} \frac{1}{\overline{x^2} - \overline{x}^2}}\,. \tag{4}$$

4. Main results

Our results for the 4 most promising examples, IC 418, NGC 2392, Hen 2-113, and NGC 1514, in which we find some evidence of magnetic signatures, are summarized in Table 1. Columns 4 and 5 give the mean longitudinal magnetic field together with the $1\,\sigma$ error found from the regression analysis, using the whole spectral range ("all lines") given in Col. 3, or using only hydrogen and helium lines, respectively. The regression detections for these central stars are illustrated in Fig. 2. The remaining 8 targets were considered non-detections.

Table 1. Regression detections of magnetic fields in PN central stars.

Target	Night	Wavelength range [Å]	$\langle B_z \rangle$ [G] all lines	$\langle B_z \rangle$ [G] H/He	$\langle B_z \rangle_{crit}$ [G]
IC 418	2	3650 – 5590	-314 ± 53	-433 ± 60	21
	3	3650 – 5590	91 ± 53	119 ± 58	
NGC 2392	1	3650 – 5590	19 ± 58	21 ± 63	28
	2	3650 – 5590	196 ± 59	220 ± 65	
Hen 2-113	1	3705 – 5768	-57 ± 15	-58 ± 23	23
	2	3705 – 5768	-98 ± 15	-165 ± 21	
NGC 1514	1	3650 – 5590	198 ± 89	168 ± 99	–
	2	3650 – 5590	-306 ± 76	-387 ± 86	

Our measurements definitely exclude the presence of large-scale (kG) magnetic fields on any of the central stars of our sample. However, we may have found evidence for the existence of weaker fields (of the order of 100 G) in the 4 targets listed in Table 1. In many cases, we could see a striking night-to-night spectral variability, which we attributed to rotational modulation.

From the basic stellar properties, including the wind parameters, we evaluated the so-called *wind magnetization parameter* [2], from which we can estimate the minimum present-day mean longitudinal magnetic field, $\langle B_z \rangle_{crit}$, that would be necessary to ensure that the stellar wind (and PN) has been shaped magnetically since early post-AGB evolution. It turns out that a rather weak field, of the order of 20 G, is actually sufficient (see Table 1, Col. 6).

5. Additional statistical tests

By using a synthetic PoWR spectrum representation for Hen 2-113 (e.g. [5]), we simulated the regression method (for $\langle B_z \rangle = 0$) for 1000 different random photon-noise realizations, assuming $S/N = 920$. The width of the resulting B-field distribution corresponded to a 1σ uncertainty of 35 G, which is about twice as large as the formal error derived from the linear regression (Table 1). The magnetic field in Hen 2-113 had therefore to exceed 100 G in order for it to be detectable with a confidence of 3σ.

In another test, we generated for each original dataset $M = 10^6$ statistical variations by bootstrapping (e.g. [12]), and analyzed the resulting distribution of M regression results. The mean $\langle B_z \rangle$ was always close to the regression result obtained from the original dataset, but the 1σ uncertainty was roughly a factor 3 larger than that given by Eq. (4), except for NGC 1514 where both error estimates

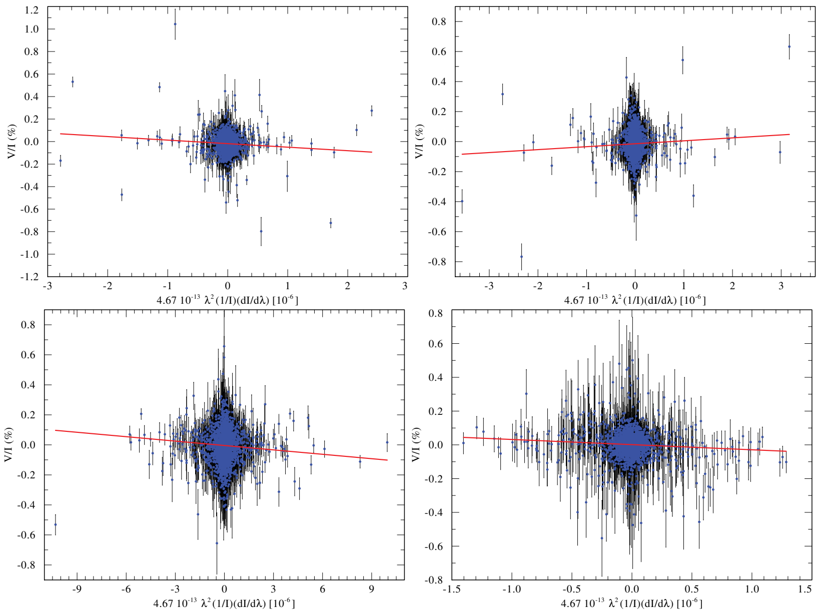

Figure 2. Regression detections for the central stars of IC 418, NGC 2392, Hen 2-113, and NGC 1514 (from *upper left* to *lower right*), using "all lines". The individual statistical errors $\sigma_i = (S/N)^{-1}$ are indicated by vertical bars.

agree.

6. Conclusions

According to the uncertainties from the standard linear regression formula (Eq. (4)), we made positive detections of magnetic fields at the 3σ significance level in three central stars: IC 418, NGC 2392, and Hen 2-113. The measured magnetic field strengths are sufficient to shape the Planetary Nebula around all three objects.

If instead we adopted the more conservative error estimates resulting from the Monte Carlo simulations, the detections in those three central stars become only marginal (1σ) detections. Only NGC 1514 remains a clear detection, but it may not be relevant to the question of magnetic PN shaping because the magnetic field that was detected belongs to the A-type companion of the central star.

Until the matter of the size of the error bars is settled, we have to conclude that, unfortunately, our measurements can neither support nor disprove the hypothesis of magnetic PN shaping.

References

1. Balick B., Frank A. 2002, ARA&A, 40, 439
2. Chevalier R. A., Luo D. 1994, ApJ, 421, 225
3. De Marco O. 2009, PASP, 121, 316
4. García-Segura G., Langer N., Różyczka M., Franco J. 1999, ApJ, 517, 767
5. Hamann W.-R., Gräfener G. 2003, A&A, 410, 993
6. Hubrig S., Kurtz D. W., Bagnulo S., et al. 2004a, A&A, 415, 661
7. Hubrig S., Szeifert T., Schöller M., et al. 2004b, A&A, 415, 685
8. Jordan S., Werner K., O'Toole S.J. 2005, A&A, 432, 273
9. Jordan S., Bagnulo S., Werner K., O'Toole S .J. 2012, A&A, 542, A64
10. Leone F., Martínez González M. J., Corradi R. L. M., et al. 2011, ApJL, 731, L33
11. Press W. H., Teukolsky S. A., Vetterling W. T., Flannery B. P. 2007, Cambridge: University Press, 3rd ed., p. 780 ff
12. Rivinius T., Szeifert T., Barrera L., et al. 2010, MNRAS, 405, L46